ρ^2, where ρ_T and ΔR are the density and thickness of the tamper]. Even though the shell should be Fermi degenerate (to minimize the energy of compression) no additional energy penalty is paid to reach such densities because the increased degeneracy energy from compression is well balanced by the decrease in material needed to attain a specific $\rho_T \Delta R$. (It is $\rho_T \Delta R$ of the tamper rather than its mass which determines the energy gain of the target[1]). Since in many target designs, the input energy varies as the compressed mass, α-particle reflection could lead to a substantial reduction in the driver energy needed to achieve thermonuclear ignition.

These arguments apply mainly to the small targets that are designed to demonstrate the feasibility of inertially confined fusion by reaching near-breakeven conditions, and not to high-gain, reactor-grade designs. It should be emphasized that α-particle reflection is only one of many mechanisms that will affect ignition, and which need further study. Others presently under investigation include: (1) reduction in thermal conduction to the tamper by intentionally seeding the fuel with high-Z ions, (2) large contamination of the fuel by high-Z tamper ions due to hydrodynamic instabilities, and (3) preheat of the fuel resulting from an incomplete understanding of energy transport in the design of the target. Of these, only high-Z seeding and α-particle reflection can relax the constraints needed for thermonuclear ignition.

This work was partially supported by the following sponsors: Exxon Research and Engineering Company, General Electric Company, Northeast Utilities Service Company, New York State Energy Research and Development Authority, The Standard Oil Company (Ohio), The University of Rochester, and Empire State Electric Energy Research Corporation.

[1]R. J. Mason and R. L. Morse, Nucl. Fusion 15, 935 (1975).

[2]J. D. Jackson, *Classical Electrodynamics* (Wiley, New York, 1962), pp. 451–459.

[3]S. Skupsky, Phys. Rev. A 16, 727 (1977).

[4]E. G. Corman, W. E. Loewe, G. E. Cooper, and A. M. Winslow, Nucl. Fusion 15, 377 (1975).

[5]G. S. Fraley, E. J. Linnebur, R. J. Mason, and R. L. Morse, Phys. Fluids 17, 474 (1974).

[6]J. Nuckolls, L. Wood, A. Thiessen, and G. Zimmerman, Nature (London) 239, 139 (1972).

Convective Plasma Loss Caused by an Ion-Cyclotron rf Field and Its Elimination by Mode Control

Y. Yasaka and R. Itatani

Department of Electronics, Kyoto University, Kyoto 606, Japan

(Received 17 September 1979)

This paper reports experimental evidence that a convective loss occurs in a low-density plasma subjected to the ion-cyclotron rf field of $m = \pm 1$ azimuthal mode which is conventionally employed. By utilization of an $m = +1$ circularly polarized rf field produced with a multiphase rf source, the convective plasma loss is eliminated, which results in an improvement in heating efficiency by more than 70%.

PACS numbers: 52.50.Gj, 52.25.Fi, 52.35.Hr

Radio frequency heating has now been recognized as one of the most promising methods for direct heating of ions in a fusion plasma. In conjunction with heating, however, there has been observed anomalous loss of the plasma due to rf-enhanced turbulence.[1,2] Recently, Wong and Bellan[3] reported the enhancement of drift waves by electric fields near the lower hybrid frequency, which results in modification of density profile. The effect of ponderomotive force also becomes important when the excursion velocity of particles in rf fields exceeds the thermal velocity. It is thus desirable not only to achieve higher heating efficiency but to reduce enhanced plasma loss during rf heating.

In this Letter, we wish to present the experimental evidence that an rf field of $m = \pm 1$ azimuthal mode, which is conventionally used in ion-cyclotron rf (ICRF) heating, produces convective cross-field plasma loss. By utilizing the $m = \pm 1$

circularly polarized rf field, we can achieve higher overall heating efficiency in consequence of eliminating convective plasma loss.

The convective loss is produced through particle drifts due to the ponderomotive force of the large-amplitude rf field. Let us consider a cylindrical, homogeneous, collisionless plasma with radius r_c immersed in a static magnetic field B_0 in the z direction. If the current density in a Kharkov-type coil[4] [see coil B in Fig. 1(a)] is approximated by $j_\theta = j_0\,\delta(r - r_a)\sin\theta\cos(-k_\parallel z + \omega t)$ with r_a being the coil radius, the rf electric field in the plasma is the superposition of fields of $m = +1$ and -1 modes, and may be represented by

$$E_r^{(1)} = [E_1(r) + E_2(r)]\cos\Phi_1 + [E_3(r) + E_4(r)]\cos\Phi_2,$$
$$E_\theta^{(1)} = [-E_1(r) + E_2(r)]\sin\Phi_1 + [-E_3(r) + E_4(r)]\sin\Phi_2,\quad E_z^{(1)} = 0, \qquad (1)$$

where $\Phi_1 = \theta - k_\parallel z + \omega t$, $\Phi_2 = -\theta - k_\parallel z + \omega t$ with $k_\parallel$ the axial wave number, and E_1 (E_3) and E_2 (E_4) are, respectively, the amplitudes of the left- and right-hand circularly polarized field components of the $m = +1$ (-1) mode. [Hereafter, the field in Eq. (1) is termed the $m = \pm 1$ field.] Following the procedure used by Chen and Etievant[5], we can obtain linear and second order (in the field amplitude) solutions for particle motions. To second order, the ponderomotive force gives rise to a quasisteady drift of ions in the direction perpendicular to both the force and $\vec{B}_0$. After some algebra, we obtain the radial component of the quasisteady ion flux, which is given by

$$\Gamma_{ir} = 2\left(\frac{e}{m_i}\right)^2 \frac{n_0}{\omega_{ci}} \frac{1}{r}\sin 2\theta \times\left[\frac{E_1 E_3}{(\omega-\omega_{ci})^2} + \frac{E_2 E_4}{(\omega+\omega_{ci})^2}\right], \qquad (2)$$

where m_i is the ion mass, n_0 is the plasma density, and ω_{ci} is the ion cyclotron angular frequency.[6] This shows that the large cross-field ion flux is produced by the $m = \pm 1$ rf field at the fundamental ion cyclotron resonance. We must note that the $m = +1$ and -1 rf fields in Eq. (1) are not necessarily the wave fields.

In order to eliminate this convective plasma loss, we design an rf coil which can produce the $m = +1$ or -1 rf field selectively. [see coil A in Fig. 1(a)] In this case, we have $E_3 = E_4 = 0$ (for the $m = +1$ mode), or $E_1 = E_2 = 0$ (for the $m = -1$ mode); then Eq. (2) predicts that no radial flux of ions is produced.

The experiments were performed in a single-ended Q machine of a potassium plasma. The plasma, with density $n_0 = (0.1 - 5)\times 10^{10}$ cm^{-3}, formed a column 4 cm in diameter and 1.3 m long in an axial uniform magnetic field up to 10 kG. For the excitation of the $m = \pm 1$ field, we use coil B with $r_a = 3$ cm and $2\pi/k_\parallel = 52$ cm set 50 cm downstream from the hot plate. (Actually, two coils are used in order to determine $k_\parallel$.) The coil is fed by an oscillator which can deliver

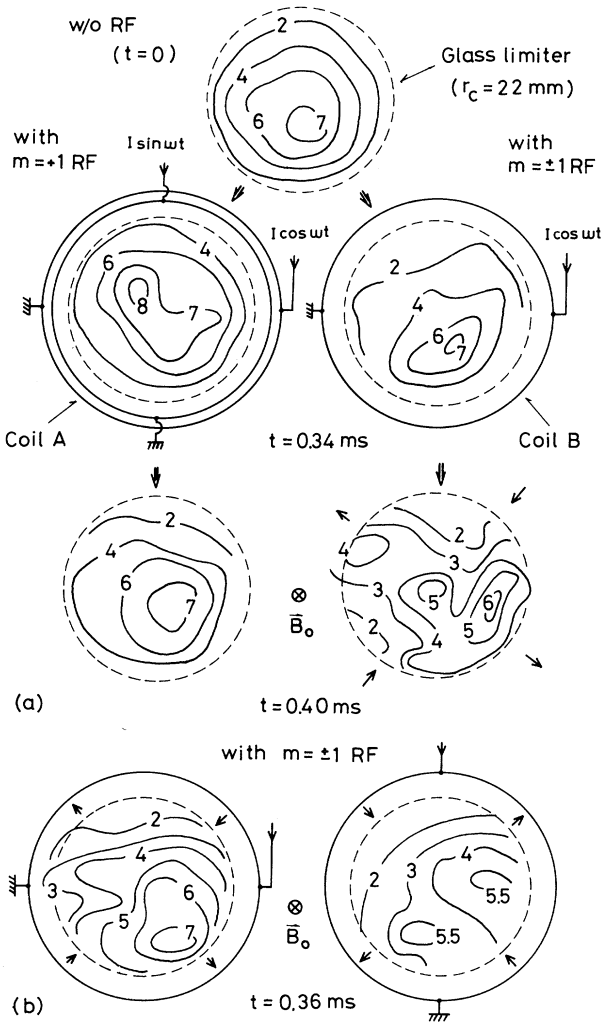

FIG. 1. Two-dimensional profiles of ion saturation current I_{is} (in arbitrary units) for $n_0(r = 0) = 1.2\times 10^{10}$ cm^{-3}, $\omega/\omega_{ci} = 0.99$, and $I_T{}^2 = 0.51\times 10^3$ A^2. A simplified schematic of the rf coils is also shown. (a) Temporal evolution of I_{is} profile for the $m = +1$ mode (left traces) and for the $m = \pm 1$ mode (right traces). (b) I_{is} profile for the $m = \pm 1$ mode with two different coil positions. The direction of Γ_{ir} predicted by Eq. (2) is indicated by arrows.

pulsed rf power up to 200 W at a frequency of 0.35 MHz. The rf coil A for the selective excitation of the $m = +1$ or -1 field simply consists of two elements displaced azimuthally by 90° each other. Each element, which has the same dimension as coil B, is connected to the oscillator through an LC phase-shifter. Driving two elements 90° out of phase, we can produce the azimuthally rotating field.

When coil A was operated in the $m = +1$ mode, the amplitude of the rf magnetic field away from the coil was resonantly peaked at $\omega/\omega_{ci} = 0.98$ for $n_0 = 2.0\times10^{10}$ cm^{-3}, and the field was almost left-hand circularly polarized on axis. When n_0 was decreased, the peak shifted closer to the point where $\omega/\omega_{ci} = 1$. For the $m = -1$ operation, the amplitude of the rf field changed little from that without the plasma, and had no dependence on ω/ω_{ci}. These results indicate that the $m = +1$ field generates the $m = +1$ slow wave, while the $m = -1$ field generates only an antenna near field rather than a propagating wave field. For the coil B, the $m = \pm 1$ field is equally divided into the $m = +1$ and -1 spectral powers, and both the $m = +1$ slow wave and the $m = -1$ antenna near field are generated.

The temporal evolution of the two-dimensional profile of ion saturation current I_{is} during an rf pulse was measured with a Langmuir probe movable in three degrees of freedom. The equal-I_{is} contours are displayed in Fig. 1(a) for the $m = +1$ and ±1 operations with mean squared rf current $I_T^2 = 0.51\times10^3\ A^2$, $\omega/\omega_{ci} = 0.99$, and $n_0 = 1.2\times10^{10}$ cm^{-3} for both modes. The contours are almost concentric at $t = 0$ (before the rf pulse) and continue to be so with time for the $m = +1$ operation. On the contrary, the profile for the $m = \pm 1$ operation shows a convective drift pattern at $t = 0.4$ msec such that higher-density, hot ions in the plasma core drift radially outward and lower-density, cold ions in the periphery radially inward in adjacent quadrants alternately. From the boundary condition which relates $B_z^{(1)}$ to j_θ, we note that the azimuthal position where $j_\theta = 0$ corresponds to $\theta = 0$ or π in the theory described before. The arrows in Fig. 1(a) designate the direction of Γ_{ir} predicted from Eq. (2). There is good agreement between the prediction and the experimental result. We note also from Eq. (2) that the rotation of the rf coil B in azimuth by 90° will result in reversal of the direction of Γ_{ir}. This is demonstrated by the difference of the measured I_{is} contours in Fig. 1(b). Only the rf coil B was rotated by 90° between the two traces; all other parameters were the same. The convective drift patterns correspond well with the theoretically predicted direction of Γ_{ir} which is again indicated by arrows. No enhanced cross-field loss was observed when the $m = -1$ field was applied, showing that both E_1 and E_3 (or E_2 and E_4) are necessary for the convective motion.

The cross-field ion flux was obtained in such a way that the axial ion saturation current I_c to the negatively biased cold end plate of radius r_p was measured as a function of axial distance z to give Γ_{ir} which is equal to $(2\pi r_p e)^{-1}(\partial I_c/\partial z)$.[7] Figure 2 shows Γ_{ir} divided by the density averaged over the cross section, $\bar{n}$, as a function of I_T^2. Drift-wave activities,[3] an increase of the amplitude and the phase velocity and changes in the frequency spectrum, were observed as I_T^2 was increased. The dotted curve in Fig. 2 is drawn theoretically with use of the Bohm diffusion coefficient with measured T_e and the density scale length for the $m = +1$ case. The numerical factor of the coefficient, so chosen as to fit the experimental data at $I_T^2 = 0$, is 5.2×10^{-2}. The theoretical curve agrees well with the experimental points for the $m = +1$ mode, showing that the increase of radial loss for this mode is due to the enhancement of Bohm diffusion. Since the drift-wave activities were nearly the same for both modes with the same I_T^2, the excess of $\Gamma_{ir}/\bar{n}$ for the $m = \pm 1$ mode (solid curve) over that of

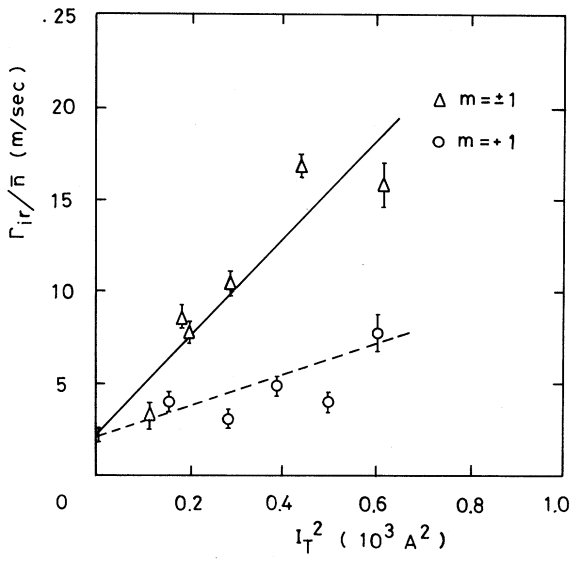

FIG. 2. Radial ion flux Γ_{ir} divided by the averaged plasma density $\bar{n}$ vs mean square rf current in the rf coil, I_T^2, for the $m = +1$ and $m = \pm 1$ modes. [$n_0 = (1\text{–}3)\times10^{10}$ cm^{-3} and $\omega/\omega_{ci} = 0.98$.]

the Bohm diffusion (dotted curve) is attributed to the radial ion convection peculiar to the $m = \pm 1$ field. This fractional $\Gamma_{ir}/\bar{n}$ corresponding to the convective loss is proportional to I_T^2, which is consistent with Eq. (2) since E_1 to E_4 are proportional to I_T. From the measurement of wave magnetic fields with probes, the magnitudes of E_1 and E_3 are estimated to be 6.3 V/m and 3.8 V/m, respectively, at $r = 2.0$ cm for $I_T^2 = 0.62 \times 10^3$ A^2. Substituting these values and $\omega/\omega_{ci} = 0.98$ into Eq. (2), we obtain $\Gamma_{ir}/\bar{n} \simeq 2\Gamma_{ir}/n_0(r=0)$ to be 6.7 m/sec with an error of $\pm 30\%$ involved in the estimation of the field amplitudes. The directly measured value of $\Gamma_{ir}/\bar{n}$ for the $m = \pm 1$ mode above the Bohm diffusion value is 6.9–9.3 m/sec for the same I_T^2 as shown in Fig. 2. The agreement between theory and experiment is seen to be very good.

There may arise a question that the convective drifts are produced by the azimuthal asymmetry of equilibrium potential due to asymmetric heating of ions or electrons by the $m = \pm 1$ field. A difference in equilibrium potential of 0.6–0.8 V between two points separated by 90° in azimuth at $r \simeq 1.5$ cm is necessary to produce $\Gamma_{ir} \simeq 9 \times 10^{15}$ m^{-2} sec^{-1}, which is measured at $\bar{n} = 0.5 \times 10^9$ cm^{-3}, $n_0(r = 1.5\ \text{cm}) = 0.3 \times 10^9$ cm^{-3}, and $I_T^2 = 0.48 \times 10^3$ A^2. However, the measured potential difference is always less than 0.3 V, which is much weaker than that required.

The ion temperature as measured with a multigrid energy analyzer was raised from 0.3 to about 20 eV for the $m = +1$ operation, while it was less than 2 eV for the $m = -1$ operation. ($I_T^2 = 9.0 \times 10^2$ A^2 for both modes.) For the $m = +1$ mode, the increment of ion energy density, Δp, is proportional to both the incident rf power and initial plasma density, provided $\omega/\omega_{ci} = 0.97$. The $\pm 10\%$ discrepancy in ω/ω_{ci} value yields the reduction of Δp by a factor of 3.

The heating efficiency for each rf mode is given in Fig. 3, where the ordinate is the maximum Δp and the abcissa is the incident rf energy into the plasma from $t = 0$ to the time when the maximum Δp is attained. The increased ion energy density is proportional to the incident rf energy. We can see that the $m = +1$ operation of the rf coil indeed improves the overall heating efficiency over the $m = \pm 1$ operation by more than 70%. From the loading measurement, we found that, in the $m = \pm 1$ operation, about 20% of the incident rf power is dissipated in the $m = -1$ field which heats ions little as shown in Fig. 3. So the elimination of the $m = -1$ field component should result in improvement in heating efficiency of no more than 20%. The observed improvement far more than expected is because of the heating by the $m = \pm 1$ field is accompanied by the convective cross-field loss of accelerated ions.

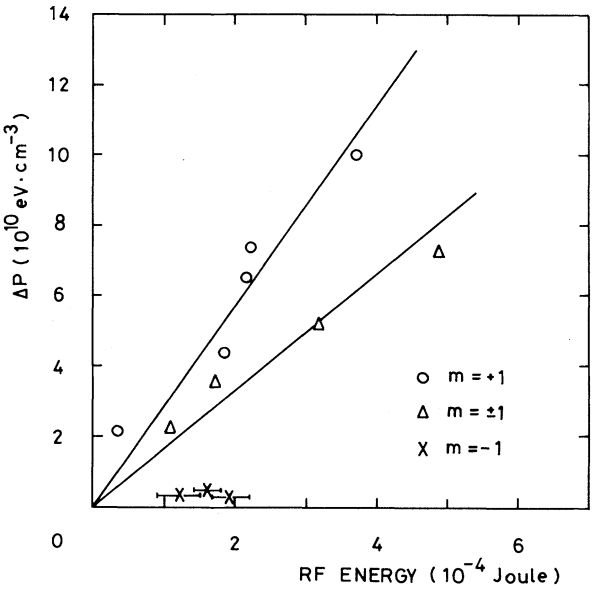

FIG. 3. Maximum increment of ion energy density vs incident rf energy for three operating modes. ($n_0 = 5.0 \times 10^{10}$ cm^{-3} and $\omega/\omega_{ci} = 0.97$.)

In summary, we have observed convective plasma loss caused by the azimuthal ponderomotive force of the $m = \pm 1$ ICRF field. This result is in quantitative agreement with the theory based on the fluid model. By utilization of the $m = +1$ circularly polarized ICRF field, the convective loss is eliminated, and an improvement in heating efficiency by more than 70% is achieved.

This work was supported by a Grant-in-Aid for Scientific Research from the Ministry of Education.

[1]S. N. Golovato and J. L. Shohet, Phys. Rev. Lett. 37, 1272 (1976).

[2]H. Hsuan *et al.*, in *Proceedings of the Third Topical Conference on Radio Frequency Plasma Heating, Pasadena, California, 1978* (Caltech, Pasadena, 1978), Paper No. C8.

[3]K. L. Wong and P. M. Bellan, Phys. Fluids 21, 841 (1978).

[4]A. G. Diky *et al.*, in *Proceedings of the Sixth European Conference on Plasma Physics and Controlled*

Fusion Research, Moscow, U.S.S.R., 1973 (Joint Institute for Nuclear Research, Moscow, 1973), p. 105.

[5]F. F. Chen and C. Etievant, Phys. Fluids 13, 687 (1970).

[6]Equation (2) is derived under the condition that the rf field is traveling in the z direction. In the case of an axially standing field, Γ_{ir} is represented by Eq. (2) multiplied by $\cos^2 k_{\parallel} z$, apart from small nonresonant terms.

[7]John A. Decker *et al.*, Phys. Fluids 10, 2442 (1967).

Evolution of Colliding Plasmas

Anthony L. Peratt

Maxwell Laboratories, Inc., San Diego, California 92123

and

James Green and Dale Nielsen[a]

Institute for Plasma Research, Stanford University, Stanford, California 94305

(Received 17 March 1980)

Three-dimensional, electromagnetic computer simulations are presented showing the evolution of colliding columnar plasmas. The interaction leads to a spiral configuration during which radiation is emitted.

PACS numbers: 52.55.Dy, 52.55.Ez, 52.65.+z, 98.50.Eb

The behavior and interaction of colliding plasmas is a problem which has been under investigation for twenty-five years. The salient point of these investigations is that plasmas which are generated and fired at each other from plasma guns or sources do not merge and decay in a simple manner. Instead, a rather dramatic configurational transformation is observed during which the emission of radiation is recorded. Bostick[1,2] first coined the term "plasmoid" to describe the magnetic-field–carrying structure which he observed and photographed. Figure 1 depicts time-resolved Kerr-cell photographs and illustrates the attraction/repulsion property of interacting plasmoids. The winding and dragging of the plasmoid's magnetic fields leads to the creation of a spiral formation.

Renewed interest in colliding plasmas is primarily due to two device-oriented research applications; fast plasma shutters for high-power glass lasers and radiation source emission from colliding exploding-wire plasmas in high-power pulseline generators. In the first case, a dense ($>10^{21}$ cm^{-3}) propagating plasma produced from an exploding wire is used to shield the final output amplifiers from target-reflected laser light. In the second case, a load consisting of an array of exploding wires is strung between the anode and cathode of a multiterawatt generator diode. X-ray pinhole-camera photographs of the radiation from the colliding vaporized-wire plasmas often show a distinct helical form. At times, dense plasma columns, or filaments, which are apparently those of the original wire plasmas,

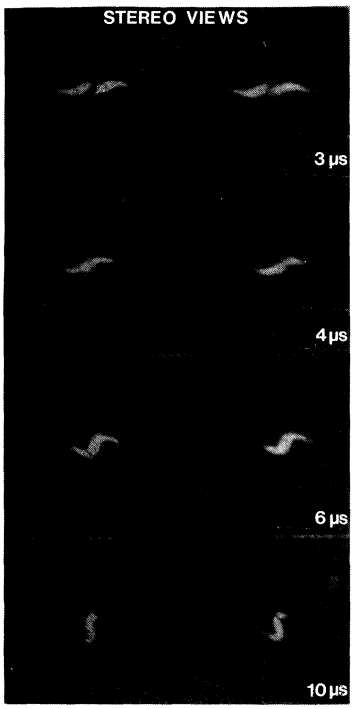

FIG. 1. Kerr-cell photographs of two plasmoids fired from sources 10 cm apart across a magnetic field of 4.7 kG (into paper) (Ref. 1).